Title: Both stem and crown mass affect tree resistance to uprooting

Authors: Tsutomu Urata[a], Masato Shibuya[*, a], Akio Koizumi[a], Hiroyuki Torita[b], JooYoung Cha[c]

[a] Graduate School of Agriculture, Hokkaido University, Sapporo 060-8589, Japan

[b] Forest Research Department, Hokkaido Research Organization, Higashiyama, Koshunai, Bibai 079-0166, Japan

[c] Northern Station of the Experimental Forest, Field Science Center for Northern Biosphere, Hokkaido University, Tokuda, Nayoro 096-0071, Japan

* **Corresponding author;** Tel & Fax: +81-11-706-3346,

E-mail: shibuya@ for.agr.hokudai.ac.jp

Address for proofs; To M. Shibuya, Graduate School of Agriculture, Hokkaido University, Sapporo 060-8589, Japan: Tel & Fax: +81-11-706-3346,

E-mail: shibuya@ for.agr.hokudai.ac.jp

Article type: Original article

Subject area and field: Biology and Ecology, Silviculture

Pages: 19 pages

Tables and Figures: 3 tables and 5 figures

Abstract

To examine the hypothesis that both stem and crown mass affect the resistance of a tree to uprooting and that tree resistance increases with the increase in crown mass, we conducted tree-pulling experiments on three *Picea glehnii* plantations (Stands A, B, and C: 27–32 years old) that differed in tree density and slenderness ratio. Allometries between crown and stem masses and between the critical uprooting moment and stem mass differed significantly among the three stands, with the crown mass and critical moment significantly larger in Stand C than in Stands A or B, despite the same stem mass. These results quantitatively verified our hypothesis. Allometries between crown and stem masses and between critical uprooting moment and stem mass were highly significant in each stand but were stand specific. Therefore, these allometries can be used to estimate tree resistance to uprooting in a given stand but not for data compiled from stands of various conditions and tree shapes. The allometry between critical moment and aboveground mass did not differ among the three *Picea* stands; thus, it is not stand specific and is generally appropriate to use for estimating tree resistance. To increase tree resistance to uprooting, we recommend light management for *Picea glehnii* plantations and probably other coniferous plantations as well.

Keywords Aboveground mass· Allometry· Critical moment· Tree density· Uprooting

Introduction

Estimating tree resistance to wind load is important in managing the risk of wind damage to coniferous plantations (Peltola et al. 1999; Gardiner and Quine 2000; Gardiner et al. 2000; Moore and Quine 2000; Cucchi et al. 2005). Major wind damage to trees includes stem failure and uprooting. Studies of tree resistance to wind damage have been both observational, after actual wind damage on plantations (Cremer et al. 1982; Savill 1983; MacCurrach 1991), and experimental, such as those that tree-pulling tests (Blackburn et al. 1988; Fredericksen et al. 1993; Gardiner et al. 1997; Moore 2000; Achim et al. 2005b; Sato et al. 2009). Tree resistance is related to diameter at breast height (DBH; Peltola et al. 1999; Torita 2009), stem mass (Blackburn et al. 1988; Gardiner et al. 2000; Nicoll et al. 2006), and slenderness ratio (Cremer et al. 1982; MacCurrach 1991; Polley 1995; Papesch et al. 1997; Peltola et al. 1999; Gardiner et al. 2000; Ancelin et al. 2004). Generally, DBH and stem mass are positively related to resistance, whereas the slenderness ratio is negatively related. However, as the slenderness ratio, which is an index of stem shape, is a ratio of tree height to DBH, it does not directly relate to tree resistance to wind damage. Factors that relate to tree resistance to uprooting are the overturning moment of a tree due to wind and self-loading and the resistive moment of the tree due to its roots; those that relate to stem failure are the bending moment of a tree due to wind and self-loading and the resistive bending moment of the stem (Koizumi 1987; Gardiner et al. 1997; Peltola et al. 1999; Moore 2000). In this study, we focused on tree resistance to uprooting.

On coniferous plantations, a small slenderness ratio closely related to low tree density and large crown size, and vice versa (Kilpatrick et al. 1981; Rollinson 1988;

Ruel 1995; Gardiner et al. 1997). Thus, the ratio of the crown size (or crown mass) to the stem size (or stem mass) of a tree with a small slenderness ratio is large compared to that of a tree with a large slenderness ratio. Wind load on a tree increases proportionally with the square of wind speed and frontal area of the crown facing the wind (Mayhead 1973; Koizumi 1987; Peltola et al. 1999; Chiba 2000). Thus, the wind load on a tree with a small slenderness ratio is greater than on one with a large slenderness ratio, given the same stem mass. However, Bergeron et al. (2009) showed that the critical turning moment of *Picea mariana* trees with the same stem mass differs depending on the slenderness ratio and that *P. mariana* trees with small slenderness ratios have larger critical turning moments than trees with large ratios. If the resistive moment of a tree to uprooting depended only on stem mass, a tree of a given stem mass with a large crown size would be less resistive to uprooting than a tree of the same stem mass with a small crown size, because the overturning moment by wind, which accounts for a large portion of the moment (Peltola and Kellomäki 1993; Papesch et al. 1997; Elie and Ruel 2005; Byrne and Mitchell 2007), increases with the increase in crown size (Koizumi 1987). However, this is not consistent with results of Bergeron et al. (2009) and many other observational studies (Cremer et al. 1982; MacCurrach 1991; Polley 1995; Ruel 1995). Hence, the resistive moment of a tree may increase with crown size (or mass) more rapidly the overturning moment loaded on the crown increases. Consequently, we hypothesized that both stem mass and crown mass significantly affect the resistive moment of a tree to uprooting and that the resistive moment of a tree increases with the increase in the crown mass, as roots sustain both stem and crown masses.

In this study, we used tree-pulling experiments to examine this hypothesis. We conducted the tree-pulling experiments in coniferous plantations of similar stand ages but with different tree densities and expected disparate allometric relationships between stem and crown masses among the stands.

Materials and methods

The tree-pulling experiments were conducted on three *Picea glehnii* plantations (Stands A, B, and C) in Uryu Experimental Forest, Hokkaido University (44° 3′–29′ N, 142° 1′–20′ E), northern Japan. Mean temperature and precipitation in Uryu Experimental Forest are approximately 3°C and 1200 mm, respectively, with more than 2 m of deep snow in winter (http://forest.fsc.hokudai.ac.jp/~exfor/UrefUr.htm). The plantations are located on flat sites of brown forest soil within about 5 km of one another. Stand ages ranged from 27 to 32 years old, with differing stand conditions. Tree densities and mean slenderness ratios were 889–2525 trees/ha and 59–88, respectively (Table 1). We sampled 10, 10, and 9 *P. glehnii* trees of representative DBH range in Stands A, B, and C, respectively.

The experiments were performed in September 2008 (Stand A) and September 2009 (Stands B and C). Stands A and C had never been thinned since their establishment. In Stand B, the experiment was conducted near the end of the third growing season after thinning, with a pre-thinning density of 3644 trees/ha. Prior to the experiment, the DBH, height, crown base height, and crown width of the sample trees were measured. Figure 1 shows the pulling system. The trees were pulled over using a hand winch (max. 30 kN) through a wire, and slings attached at about 2-m height on stems of the sample trees and at stem collar of an anchor tree 7–16 m from the sample trees. Pulling height ranged from 1.4 to 2.4 m to avoid stem failure. Pulling load was measured using a load cell (max. 50kN) connected between a sling attached to the stem and the wire. Stem displacement was measured using a displacement sensor (DTP-D-500S; Kyowa, Tokyo, Japan) attached 1 m high on the opposite side of the stem from the source of the pulling. The pulling load and stem displacement were recorded using a data logger (TC-31K; Tokyo Sokki Kenkyujo, Tokyo, Japan). We estimated the horizontal stem displacement at the pulling height and the center of gravity of the aboveground part of the tree from the displacement sensor data assuming a negligible stem bend, as the pulling heights (1.4–2.4 m) and gravity centers (2.4–5.6 m) were low in all sample trees.

After being pulled, the trees were cut down at ground level and logged at 0.5-m intervals. Branches with needles were separated from the stem and weighed. Each stem section was also weighed. We estimated the center of gravity of the aboveground part and wind load from the green mass and height of each section (Byrne and Mitchell 2007).

The critical uprooting moment of the tree was estimated using the following equation (Achim et al. 2005a, 2005b; Elie and Ruel 2005; Nicoll et al. 2005; Bergeron et al. 2009):

$$M_C = M_W + M_S \qquad (1)$$

M_C, M_W, and M_S are the critical moment and the moments of pulling load and self-loading, respectively. The pulling load moment is the sum of its horizontal and vertical components (Eq. [2]; Meunier et al. 2002; Achim et al. 2005a, 2005b; Nicoll et al. 2005).

$$M_W = H_L F \cos\theta_L + \delta_L F \sin\theta_L \qquad (2)$$

M_W is the moment of pulling load (Nm), H_L is the pulling height (m), F is the pulling load (N), and θ_L and δ_L are the angle of pulling and horizontal displacement of the stem at pulling height, respectively (Fig. 1). Eq. (3) estimates the self-loading moment:

$$M_S = \delta_G W_T g \qquad (3).$$

M_S, δ_G, W_T, and g are the self-loading moment, horizontal stem displacement at the center of gravity of the aboveground part, aboveground mass, and gravity (9.8 m/s^2), respectively.

We assumed an allometric relationship between M_C and tree dimension, as several previous studies have analyzed tree resistance to uprooting using allometries with DBH (Moore 2000; Koizumi et al. 2007; Sato et al. 2009; Torita 2009), including a simple linear model using DBH (Papesch et al. 1997) and stem mass (Fredericksen et al. 1993; Achim et al. 2005b; Elie and Ruel 2005; Nicoll et al. 2006; Byrne and Mitchell 2007). The allometry, a power function $\left(y = ax^b\right)$, is a general model that includes a simple linear model (b = 1). We analyzed differences in allometries between crown and stem masses, M_C and stem mass, and M_C and aboveground mass of the sample trees of the three stands by comparing linear regressions of the standardized major axis regression after logarithmic transformation. These analyses were performed using the freeware program (s)matr (Falster et al. 2006).

To quantitatively examine tree resistance to uprooting, we estimated the critical wind speed of uprooting the sample trees from M_W (Eq. [2]; Achim et al. 2005b), which is related to wind speed and the frontal area of a crown facing the wind as follows (Mayhead 1973; Koizumi 1987):

$$M_W = \frac{1}{2}\rho C_D v^2 A H_W \qquad (4)$$

where ρ is air density (1.225 kg/m^3), C_D is drag coefficient, v is wind speed at the center of gravity, A is frontal area of the crown facing the wind, and H_W is the height of the center of the wind load. Therefore, the critical wind speed (V_C) is

$$V_C = \sqrt{\frac{2M_W}{\rho C_D A H_W}} \qquad (5)$$

in which C_D, which is species specific, asymptotically decreases with wind speed (Mayhead 1973; Rundnucki et al. 2004). Although C_D of *Picea glehnii* has not been investigated, we used C_D = 0.35, which has been determined for the congeneric species *Picea sitchensis* (Mayhead 1973), at v = 30.5 m/s. The frontal area of the crown was estimated assuming that the crown was a triangle consisting of the crown diameter perpendicular to the pulling direction and crown length. Furthermore, we assumed that the wind (V_C) affected on H_W statically, not turbulently.

Correlation analyses between V_C and tree-shape factors such as slenderness ratio, the relative height of the center of the wind load (H_W/H), crown mass/stem mass ratio, and crown length/tree height ratio, were run using the product-moment correlation coefficient. Curve fitting was performed based on the relationship between the ratio of self-loading to the critical moment of the tree and slenderness ratio. These analyses were preformed using the R software package (R Development Core Team 2008).

Results

DBH of sample trees was 10.40–18.70 cm, 10.70–15.15 cm, and 13.35–17.95 cm in Stands A, B, and C, respectively (Table 2). Heights and slenderness ratios were 11.10–14.20 m and 73–113, 9.51–11.42 m and 71–89, and 7.74–10.7 m and 57–77 in Stands A, B, and C, respectively (Table 2). The slenderness ratios of sample trees tended to descend in the order Stand A > B > C.

In pulling experiments, tree moments increased with the degree of tree leaning (Fig. 2). M_C occurred simultaneously with the maximum pulling load of some trees (Fig. 2a) and after the maximum load of other trees because of the increase in self-loading (Fig. 2b, c). Ranges of M_C were 3.228–24.320 kNm, 3.785–12.998 kNm, and 7.037–29.016 kNm in Stands A, B, and C, respectively (Table 2).

Allometries between W_C and W_S were significant for all stands (Table 3, Fig. 3a). Regression coefficients did not differ among the stands, but the Stand C intercept was significantly larger than those of Stands A and B (Table 3). The same relationship was found in allometries between M_C and W_S. Although regression coefficients for M_C–W_S allometries did not differ among the stands, the Stand C intercept was significantly larger than those of Stands A and B (Table 3, Fig. 3b). Unlike the other allometries, neither M_C–W_T regression coefficients nor intercepts differed among the stands (Table 3, Fig. 3c). Hence, a common M_C–W_T allometry among the stands could be determined. The pooled data (n=29) yielded the following allometry between M_C and W_T:

$$M_C = 1.39 \times 10^{-2} W_T^{\ 1.39} \qquad \left(r^2 = 0.88, p < 0.001\right) \qquad (6)$$

The power term differed significantly from 1 ($p < 0.001$), and M_C increased with the increase in W_T more rapidly than did the linearity.

The critical wind speed, V_C, correlated negatively with slenderness ratio (r = -0.89, $p < 0.001$; Fig. 4a) and relative height of the center of the wind load (r = -0.73, $p < 0.001$; Fig. 4b) based on the pooled data. V_C correlated positively with crown mass/stem mass ratio (r = 0.74, $p < 0.001$; Fig. 4c) and crown length/tree height ratio (r = 0.59, $p < 0.001$; Fig. 4d).

The ratio of self-loading to the critical moment of trees increased asymptotically with slenderness ratio (Fig. 5).

Discussion

Allometries between W_C and W_S and between M_C and W_S differed significantly among the three *Picea glehnii* stands studied here, with both allometries showing the same relationships among the stands (Table 3, Fig. 3). In Stand C, W_C and M_C were significantly larger for the same stem mass than in Stands A and B. We also verified our hypothesis that both stem and crown mass affect tree resistive moment to uprooting (M_C) both quantitatively and substantively. Thus, we conclude that trees with a large crown are more resistant to uprooting than those with a small crown given the same stem mass. The positive correlations between V_C and crown mass/stem mass ratio and V_C and crown length/tree height ratio (Fig. 4) also support our conclusion. As a large crown size is closely related to reduced tree density and a small slenderness ratio (Kilpatrick et al. 1981; Rollinson 1988; Ruel 1995; Gardiner et al. 1997), we recommend light management of *P. glehnii* plantations to increase tree resistance to uprooting. This recommendation most likely can be applied to other coniferous plantations, as shown in many observational studies in Europe, North America, and New Zealand (Cremer et al. 1982; Savill 1983; MacCarrach 1991; Polley 1995; Ruel 1995). The W_C–W_S and M_C–W_S allometries of each stand were highly significant (Table 3) but were stand specific. Although they are appropriate for use in estimating tree resistance to uprooting in a given stand, they should not be used with stands of various conditions and tree shapes. In these cases, the estimation of M_C from W_T is appropriate, as the M_C–W_T allometry is not stand specific (Fig. 3c). We also consider the estimation of M_C from DBH or (DBH^2 × height) to be stand specific, as relationships between DBH or (DBH^2 × height) and crown or leaf mass are generally stand specific (Shinozaki et al. 1964; Kira and Shidei 1967; Oohata 1991). Allometries between Stands A and B did not differ (Fig. 3) owing to small differences in tree density and tree slenderness ratios (Tables 1 and 2).

It is important to note that the power term W_T in Eq. (6) is significantly larger than 1. Consequently, M_C increases rapidly with W_T, resulting in larger resistance to uprooting of a large-crown tree than a small-crown tree.

The estimate of V_C is not accurate, as it is based on assumptions that *P. glehnii* C_D = 0.35; that trees do not interact with neighboring trees; and that wind affects a tree statically, as in a pulling experiment, not turbulently. However, the estimate is appropriate for evaluating tree resistance to uprooting, as it includes the influences of both crown mass on M_C and wind load on the turning moment of a tree. The trend in V_C (Fig. 4) is consistent with observational results that trees with small slenderness ratios and large crowns (i.e. small H_W/H ratio, large crown mass/stem mass and crown length/tree height ratios) are more resistant to uprooting (Cremer et al. 1982; Savil 1983; MacCurrach 1991).

In this study, M_C consisted of the pulling load and self-loading (Eq. [1]). M_C occurred simultaneously with the maximum pulling load of some trees and after the maximum load of others (Fig. 2). Previous studies have also found these M_C occurrence patterns (Coutts 1986; Papesch et al. 1997), although the ratios of self-loading moments to M_C differed between the studies. In our study, the ratio of self-loading to M_C increased asymptotically with tree slenderness ratio (Fig. 5), and the M_C occurrence patterns may be affected by the slenderness ratio. Although we assumed that the stem bend was negligible in the estimation of the self-loading in this study, it is important to examine the stem bend and vertical variation of wind load in the estimation of self-loading

(Ancelin et al. 2004).

Elaborate mechanistic models of wind damage to trees and stands, such as ForestGALES and HWIND, have developed in Europe (Gardiner and Quine 2000; Gardiner et al. 2000; Moore and Quine 2000). Quantitative analyses of these models are necessary for wind damage risk management (Gardiner and Quine 2000). The critical moment for uprooting is assumed to be linear to stem mass in ForestGALES and to mass and depth of root–soil plate in HWIND (Peltola and Kelloäki 1993; Gardiner et al. 2000). However, such critical moments may possibly be stand specific, and, based on our results, we conclude that the method of estimating the critical moment from aboveground mass of trees is superior. The results shown in Figure 3 contribute to improving stand management simulations of coniferous plantations in relation to tree shape and wind damage risk management.

References

Achim A, Ruel J-C, Gardiner BA (2005a) Evaluating the effect of precommercial thinning on the resistance of balsam fir to windthrow through experimentation, modeling, and development of simple indices. Can J For Res 35: 1844–1853

Achim A, Ruel J-C, Gardiner BA, Laflamme G., Meunier S (2005b) Modelling the vulnerability of balsam fir forests to wind damage. For Ecol Manage 204: 35–50

Ancelin P, Courbaud B, Fourcaud T (2004) Development of an individual tree-based mechanical model to predict wind damage within forest stands. For Ecol Manage 203: 101–121

Bergeron C, Ruel J-C, Elie J-G, Mitchell SJ (2009) Root anchorage and stem strength of black spruce (*Picea mariana*) trees in regular and irregular stands. Forestry 82: 29–41

Blackburn P, Petty JA (1988) Theoretical calculations of the influence of spacing on stand stability. Forestry 61: 235–244

Byrne KE, Mitchell SJ (2007) Overturning resistance of western redcedar and western hemlock in mixed-species stands in coastal British Columbia. Can J For Res 37: 931–939

Chiba Y (2000) Modelling stem breakage caused by typhoons in plantation *Cryptomeria japonica* forests. For Ecol Manage 135: 123–131

Coutts MP (1986) Components of tree stability in Sitka spruce on peaty gley soil. Forestry 59: 173–179

Cremer KW, Borough CJ, McKinnel FH, Carter PR (1982) Effects of stocking and thinning on wind damage in plantations. New Zealand J For Sci 12: 244–268

Cucchi V, Meredieu C, Stokes A, Coligny F, Suarez J, Gardiner B (2005) Modeling the windthrow risk for simulated forest stands of Maritime pine (*Pinus pinaster* Ait.). For Ecol Manage 213: 184–196

Elie J-G, Ruel J-C (2005) Windthrow hazard modeling in boreal forests of black spruce and jack pine. Can J For Res 35: 2655–2663

Falster DS, Warton DI, Wright IJ (2006) SMATR: Standardised major axis tests and routines, ver 2.0. http://www.bio.mq.edu.au/ecology/SMATR

Fredericksen TS, Hedden RL, Williams SA (1993) Testing loblolly pine wind firmness with simulated wind stress. Can J For Res 23: 1760–1765

Gardiner BA, Quine CP (2000) Management of forests to reduce the risk of abiotic damage – a review with particular reference to the effects of strong winds. For Ecol Manage 135: 261–277

Gardiner BA, Peltola H, Kellomäki S (2000) Comparison of two models for predicting the critical wind speeds required to damage coniferous trees. Ecol Model 129: 1–23

Gardiner BA, Stacey GR, Belcher RE, Wood CJ (1997) Field and wind tunnel assessments of the implications of respacing and thinning for tree stability. Forestry 70: 233–252

Kilpatrick DJ, Sanderson JM, Savill PS (1981) The influence of five early respacing treatments on the growth of Sitka spruce. Forestry 54: 17–29

Kira T, Shidei T (1967) Primary production and turnover of organic matter in different forest ecosystems of the western Pacific. Jpn J Ecol 17: 70–87

Koizumi A (1987) Studies on the estimation of the mechanical properties of standing trees by non-destructive bending test. Res Bull Coll Exp For Hokkaido Univ 44:

1329–1415 (in Japanese)

Koizumi A, Oonuma N, Sasaki Y, Takahashi K (2007) Difference in uprooting resistance among coniferous species planted in soils of volcanic origin. J For Res 12: 237–242

MacCurrach RS (1991) Spacing: an option for reducing storm damage. Scot For 45: 285–297

Mayhead GJ (1973) Some drag coefficients for British forest trees derived wind tunnel studies. Agr Meteol 12: 123–130

Meunier S, Ruel J-C, Laflamme G, Achim A (2002) Résistance comparée de l'éopinette blanche et du sapin baumier au renversement. Can J For Res 32: 642–652

Moore JR (2000) Differences in maximum resistive bending moments of *Pinus radiata* trees grown on a range of soil types. For Ecol Manage 135: 63–71

Moore J, Quine CP (2000) A comparison of the relative risk of wind damage to planted forests in Border Forest Park, Great Britain, and the Central North Island, New Zealand. For Ecol Manage 135: 345–353

Nicoll BC, Achim A, Mochan S, Gardiner BA (2005) Does steep terrain influence tree stability? A field investigation. Can J For Res 35: 2360–2367

Nicoll BC, Gardiner BA, Rayner B, Peace AJ (2006) Anchorage of coniferous trees in relation to species, soil type, and rooting depth. Can J For Res 36: 1871–1883

Oohata S (1991) A study to estimate the forest biomass –a non-cutting method to use the piled data–. Bull Kyoto Univ For 63: 23–36 (in Japanese)

Papesch AJG, Moore JR, Hawke AE (1997) Mechanical stability of *Pinus radiata* trees at Eyrewell Forest investigated using static tests. New Zealand J For Sci 27: 188–204

Peltola H, Kellomäki S (1993) A mechanistic model for calculating windthrow and stem breakage of Scots pines at stand edge. Silva Fenn 27: 99–111

Peltola H, Kellomäki S, Väisänen H, Ikonen V-P (1999) A mechanistic model for assessing the risk of wind and snow damage to single trees and stands of Scots pine, Norway spruce, and birch. Can J For Res 29: 647–661

Polley VH (1995) Beurteilung der mechanischen Stabilität der Waldbäume auf der Grundlage der Bundeswaldinventur. Forst und Holz 50: 594–597

R Development Core Team (2008) R: A language and environment for statistics computing. R Foundation for Statistical Computing. Vienna, Austria. http://www.R-project.org

Rollinson TJD (1988) Respacing Sitka spruce. Forestry 61: 1–22

Rundnicki M, Mitchell SJ, Novak MD (2004) Wind tunnel measurements of crown streamlining and drag relationships for three conifer species. Can J For Res 34: 666–676

Ruel J-C (1995) Understanding windthrow: silvicultural implications. For Chron 71: 434–445

Sato H, Torita H, Masaka K, Kon H, Shibuya M (2009) Analysis of windthrow factors in windbreaks: In the case of Bibai, Hokkaido by typhoon No. 18 in 2004. J Jpn For Soc 91: 307–312 (in Japanese)

Savill PS (1983) Silviculture in windy climates. For Abst 44: 473–488

Shinozaki K, Yoda K, Hozumi K, Kira T (1964) A quantitative analysis of plant form–the pipe model theory II. Further evidence of the theory and its application in forest ecology. Jpn J Ecol 14: 133–139

Torita H (2009) Mechanical evaluation of the Japanese larch for wind damage. J Jpn

For Soc 91: 120–124 (in Japanese)

Figure legends

Fig. 1 Winching system used in tree-pulling experiments. Displacement sensor is 1 m from ground level. *F*: pulling load (N), H_G: height of the center of gravity of the aboveground part of the sample tree (m), H_L: pulling height (m), H_W: height of the center of gravity of the wind load (m), W_T: aboveground mass (kg), δ_L: horizontal displacement at pulling height, δ_G: horizontal displacement of the center of gravity of the aboveground part, θ_L: angle of pulling, θ_G: stem gradient.

Fig. 2 Moment of a tree with a leaning stem. Thick line: total moment; thin line: pulling load moment; dotted line: self-loading moment. Arrows indicate the maximum pulling load moment.

Fig. 3 Allometries between **(a)** crown mass (W_C) and stem mass (W_S), **(b)** critical moment (M_C) and stem mass, and **(c)** critical moment and aboveground mass (W_T). ◊: Stand A, Δ: Stand B, ○: Stand C. Solid, broken, and dotted lines are standardized major axis regressions for Stands A, B, and C, respectively.

Fig. 4 Relationships between **(a)** critical wind speed for uprooting (V_C) and slenderness ratio, **(b)** critical wind speed and relative height of the center of the wind load (H_W/H), **(c)** critical wind speed and crown mass/stem mass ratio, and **(d)** critical wind speed and crown length/tree height ratio. *r*: product-moment correlation coefficient; ***: $p < 0.001$.

Fig. 5 Relationship between self-loading ratio to critical moment and slenderness ratio. ◊: Stand A, Δ: Stand B, ○: Stand C. Fitted curve: $y = -0.00294x^2 + 0.651x - 19.8 \quad (r^2 = 0.46, p < 0.001)$.

Table 1 Stand condition

Stand	Age (years)	Density (trees/ha)	H* (m)	DBH* (cm)	Slenderness ratio*
A	32	2525	12.4±1.8	14.3±3.0	88±13
B	31	1778	9.6±2.1	12.3±3.1	80±9
C	27	889	10.3±1.7	17.7±2.9	59±7

Abbreviations; H: height, DBH: diameter at breast height.

* Mean±SD.

Table 2 Outline of sample trees by stand

Stand	H (m)	DBH (cm)	Slenderness ratio	W_S (kg)	W_C (kg)	M_C (kNm)	V_C (m/s)
A	11.10–14.20	10.40–18.70	75–113	37.7–153.6	9.6–53.4	3.228–24.320	14.8–24.8
B	9.51–11.42	11.35–15.15	71–89	38.1–84.8	14.1–43.3	3.785–12.998	17.1–29.0
C	7.74–10.97	13.35–17.95	57–77	48.9–121.0	31.9–104.5	7.037–29.016	23.8–35.2

Values indicate the range (Min.–Max.).

Abbreviations; H: height, DBH: diameter at breast height, W_S: stem mass, W_C: crown mass, M_C: critical uprooting moment, V_C: critical wind speed.

Table 3 Compariosn of allometries among stands

y	x	Stand	Regression coefficient	Intercept	r^2	Common slope	Corrected intercept
W_C	W_S	A	1.42^{ns}	-1.23^{a}	0.86^{***}	1.28	-0.97
		B	1.16^{ns}	-0.66^{a}	0.86^{***}		-0.87
		C	1.27^{ns}	-0.61^{b}	0.78^{***}		-0.63
M_C	W_S	A	1.51^{ns}	-1.90^{a}	0.95^{***}	1.48	-1.83
		B	1.32^{ns}	-1.54^{a}	0.66^{***}		-1.81
		C	1.43^{ns}	-1.57^{b}	0.82^{***}		-1.66
M_C	W_T	A	1.39^{ns}	-1.86^{ns}	0.93^{***}	1.36	-1.80
		B	1.28^{ns}	-1.67^{ns}	0.62^{***}		-1.82
		C	1.33^{ns}	-1.71^{ns}	0.81^{***}		-1.78

Allometry: $\log y = a + b \log x$.

Superscripts: Different superscripts indicate significant differences ($p < 0.05$).

^{ns}: non-significant.

Abbreviations; W_C: crown mass (kg), W_S: stem mass (kg), M_C: critical uprooting moment (kNm), W_T: aboveground mass (kg).

***: $p < 0.001$.

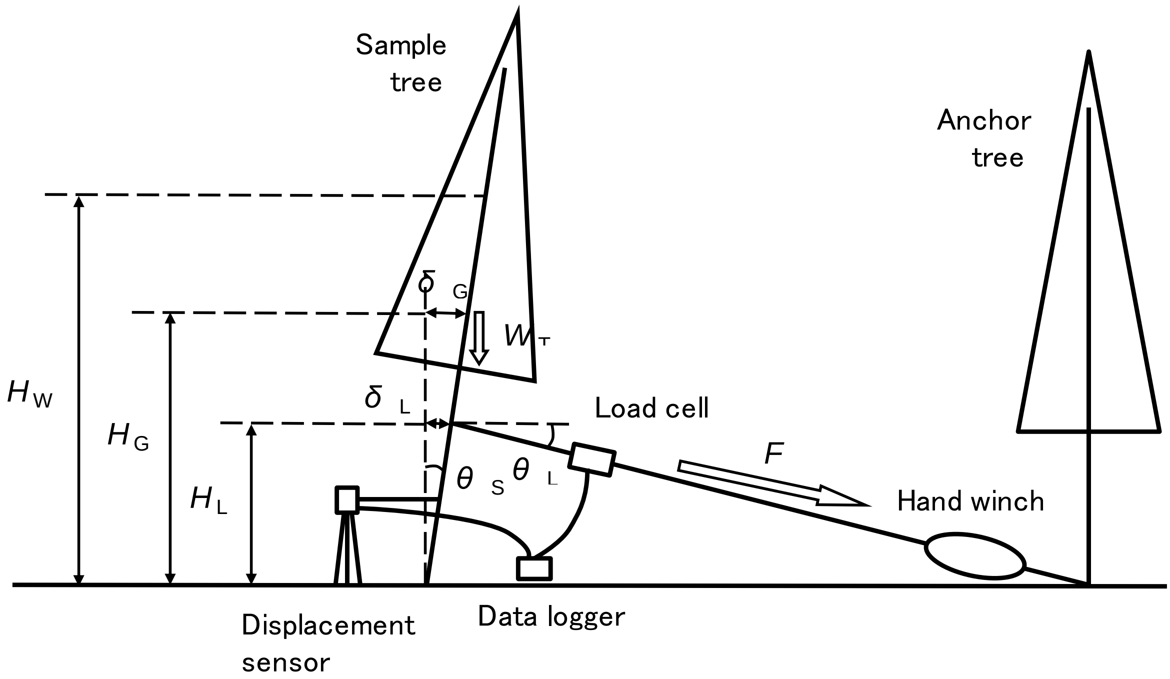

Fig. 1 Winching system used in tree-pulling experiments. Displacement sensor is 1 m from ground level. F: pulling load (N), H_G: height of the center of gravity of the aboveground part of the sample tree (m), H_L: pulling height (m), H_W: height of the center of gravity of the wind load (m), W_T: aboveground mass (kg), δ_L: horizontal displacement at pulling height, δ_G: horizontal displacement of the center of gravity of the aboveground part, θ_L: angle of pulling, θ_G: stem gradient.

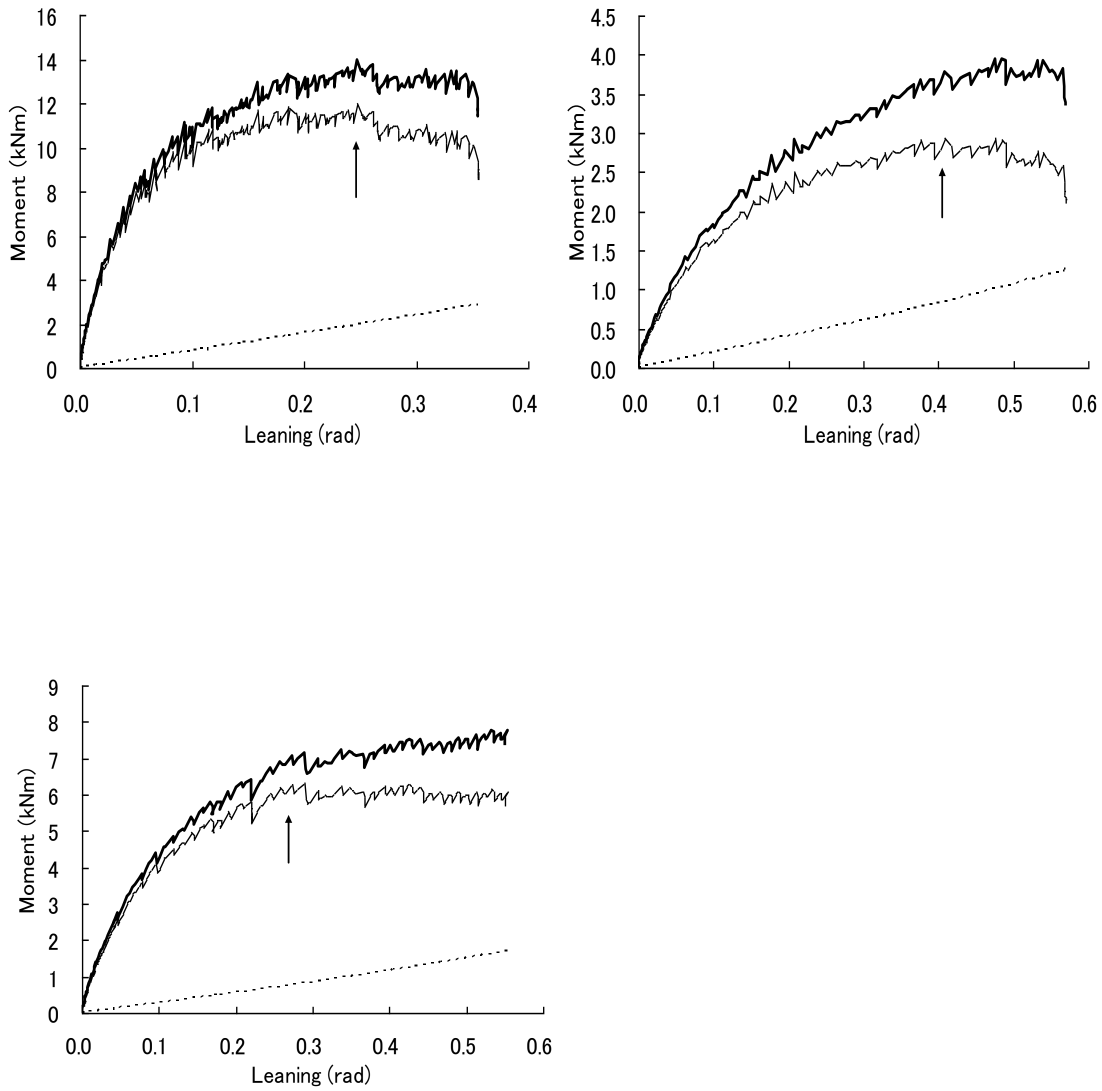

Fig. 2 Moment of a tree with a leaning stem. Thick line: total moment; thin line: pulling load moment; dotted line: self-loading moment. Arrows indicate the maximum pulling load moment.

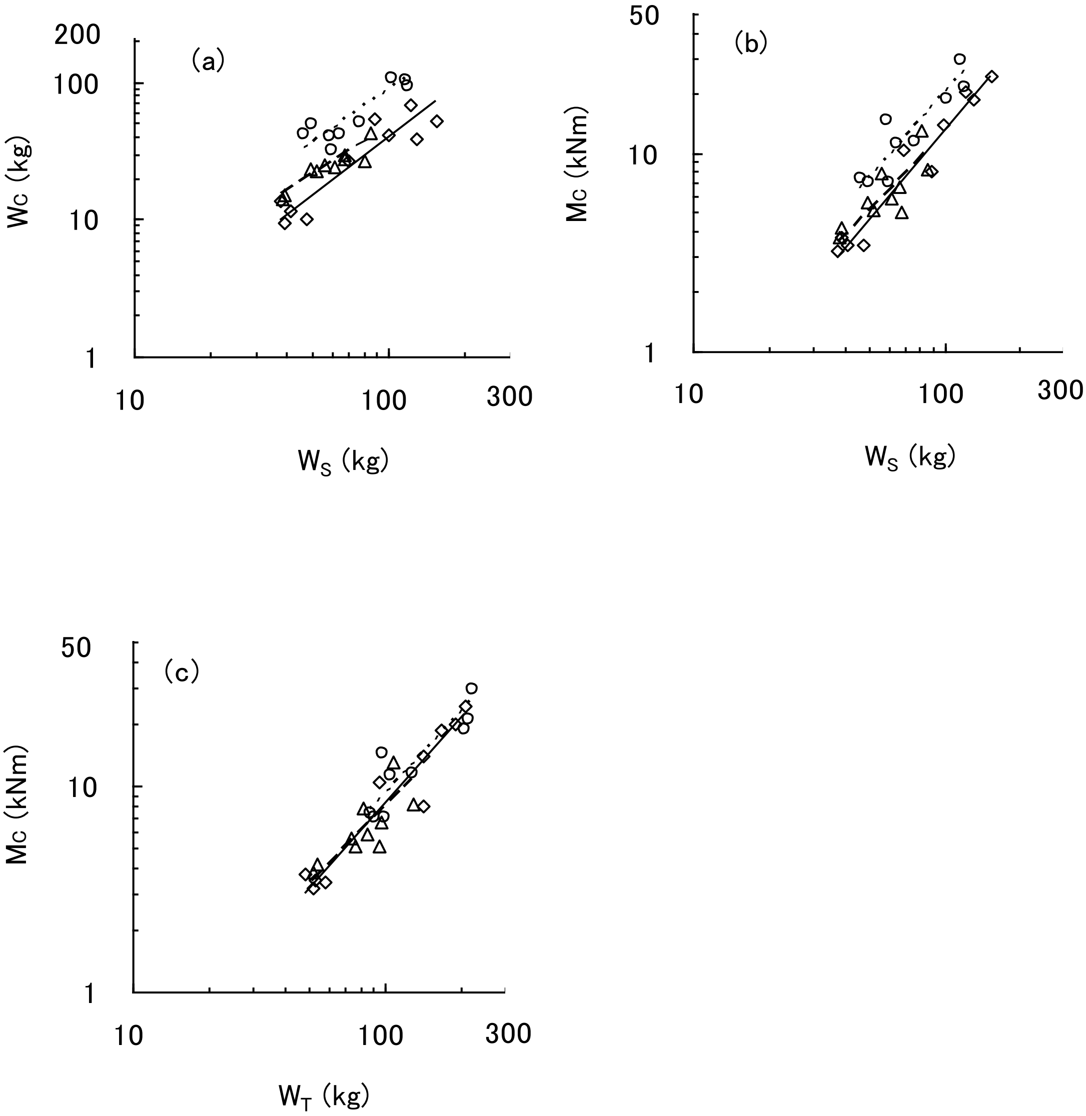

Fig. 3 Allometries between **(a)** crown mass (W_C) and stem mass (W_S), **(b)** critical moment (M_C) and stem mass, and **(c)** critical moment and aboveground mass (W_T). ◊: Stand A, Δ: Stand B, ○: Stand C. Solid, broken, and dotted lines are standardized major axis regressions for Stands A, B, and C, respectively.

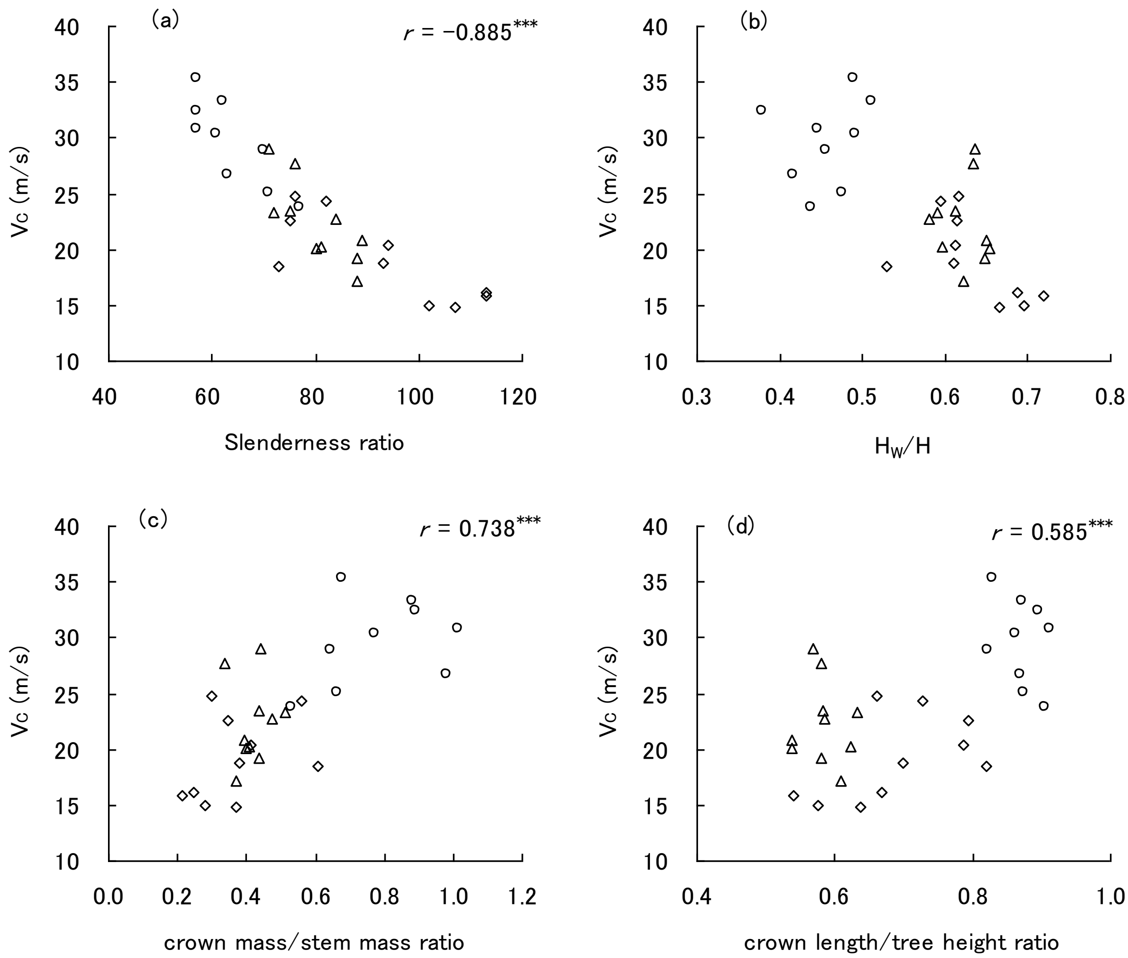

Fig. 4 Relationships between **(a)** critical wind speed for uprooting (V_C) and slenderness ratio, **(b)** critical wind speed and relative height of the center of the wind load (H_W/H), **(c)** critical wind speed and crown mass/stem mass ratio, and **(d)** critical wind speed and crown length/tree height ratio. *r*: product-moment correlation coefficient; ***: $p < 0.001$.

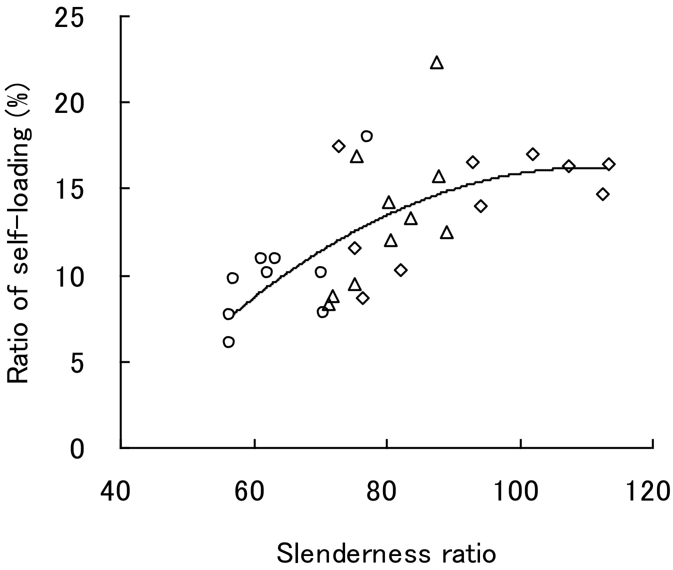

Fig. 5 Relationship between self-loading ratio to critical moment and slenderness ratio. ◊: Stand A, Δ: Stand B, ○: Stand C. Fitted curve: $y = -0.00294x^2 + 0.651x - 19.8 \quad (r^2 = 0.46, p < 0.001)$.